Group Project 1: American Options

STA2503H: Applied Probability for Mathematical Finance

Authors:

John Ndolo: 1009482560

Xinyue Xiang: 1000802973

Zhi Ye Luan: 100428267

Master of Financial Insurance

Department of Statistical Sciences,
FACULTY OF ARTS & SCIENCE

October 19, 2022

Abstract

Asset pricing is one of the critical areas in mathematics finance. This projects entails the pricing strategy of an American put option by first understanding the distributions and mathematics behind the pricing strategy and then the implementation of the pricing process. The first part entails derivation of the limiting distributions of asset price process as the number of sub-periods approaches infinity($N \to \infty$) under the physical probabilities ($\mathbb{P}$). In the second part we apply the Fundamental Theorem of asset pricing and assumptions of an arbitrage-free market in deriving the probabilities($\mathbb{Q}$ & $\mathbb{Q}^s$) under the interchange of the pair of numeraire assets (**B** and **S**) given in the problem. We further explore the limiting distributions of the respective assets as $N \to \infty$ using the derived probabilities. Lastly, we implement the pricing process of an American option in python using the binomial trees and obtain a hedging strategy at various times. We then simulate various paths the tree and obtain the implications it has on profits and loss and time of exercise by estimating the respective kernel densities and observed how differing market conditions affect these kernel densities.

Contents

1 Introduction **1**

2 Methodology **1**

2.1 Evaluating the Limiting distribution of $X^{(N)}$ under $\mathbb{P}$ 1

2.2 Distribution of S_T under probabilities $\mathbb{Q}$ and $\mathbb{Q}^s$ 3

3 Results **6**

3.1 Implementation of the American Put option 6

4 Conclusion **18**

1 Introduction

The difference between European options and American options is that, European options are exercised at maturity date while the American options can be exercised at any time up to and including maturity date. The difference between the two options means their pricing strategies are slightly different. Generally, an American put option provides the option holder with the right to sell an asset at a strike price **K** at any time up to and including the maturity date denoted by **T**. In this project, we concentrated on pricing an American put option.

The first part evaluates the limiting distribution of the given asset S_t under the physical probability measure $\mathbb{P}$. Then, by application of the concept of Fundamental Theorem of asset pricing and assumptions made under arbitrage free market, we determine the probability measures using the asset (S_t) and the risk-free asset (B_t) as a numeraire.

Finally, we discuss and summarize the findings from our exploration of the implementation for American put options in Python on how different market conditions lead to differing times of exercise and profits at time of exercise.

2 Methodology

In this problem, we considered an asset price process S denoted as $S = (S_{t_k})_{k\in\{0,1,\cdots,N\}}$, (with $t_k = k\Delta t$ and $\Delta t = \frac{T}{N}$ for a fixed N) given by a stochastic dynamic defined as;

$$S_{t_k} = S_{t_{k-1}} e^{r\Delta t + \sigma\sqrt{\Delta_t}\epsilon_k},$$

where $\epsilon_k = \{-1, +1\}$ are iid random variables and $\exists$ probability measure $\mathbb{P}$ given as

$$\mathbb{P}(\epsilon_t = \pm 1) = \frac{1}{2}\big(1 \pm \frac{(\mu - r) - \frac{1}{2}\sigma^2}{\sigma}\sqrt{\Delta t}\big),$$

where $r \geq 0$ and $\sigma \geq 0$ are some constants. Moreover, we defined a standard bank account as $B = (B_{t_k})_{k\in\{0,1,\cdots,N\}}$, with

$$B = e^{rt}.$$

2.1 Evaluating the Limiting distribution of $X^{(N)}$ under $\mathbb{P}$

Let $X^{(N)}$ denote the random variable $X^{(N)} := \log(\frac{S_T}{S_0})$. We want to prove that

$$X^{(N)} \xrightarrow[N\to\infty]{d} (\mu - \frac{1}{2}\sigma^2)T + \sigma\sqrt{T}Z,$$

where $Z \overset{\mathbb{P}}{\sim} \mathcal{N}(0, 1)$.

Proof. We want to show the limiting distribution of the process $X^{(N)}$ under the physical probability $\mathbb{P}$ as number of sub-periods approaches infinity. By generalization, we know that,

$$\begin{aligned} S_T &= S_0 e^{rN\Delta t+\sigma\sqrt{\Delta t}\sum_{k=1}^{N}\epsilon_k} \\ \frac{S_T}{S_0} &= e^{rN\Delta t+\sigma\sqrt{\Delta t}\sum_{k=1}^{N}\epsilon_k} \end{aligned}$$

Hence the definition of , $X^{(N)} := log(\frac{S_T}{S_0} = rN\Delta t + \sigma\sqrt{\Delta t}\sum_{k=1}^{N}\epsilon_k$.

NOTE: Given the probability Mass function(PMF) of ϵ_k, we can derive $\mathbb{E}^{\mathbb{P}}(\epsilon_k)$, as

$$\begin{aligned} \mathbb{E}^{\mathbb{P}}(\epsilon_k) &= \frac{1}{2}\Big[\Big(1+\frac{(\mu-r)-\frac{1}{2}\sigma^2}{\sigma}\sqrt{\Delta t}\Big)-\Big(1-\frac{(\mu-r)-\frac{1}{2}\sigma^2}{\sigma}\sqrt{\Delta t}\Big)\Big] \\ &= \frac{(\mu-r)-\frac{1}{2}\sigma^2}{\sigma}\sqrt{\Delta t} \end{aligned}$$

and $\mathbb{E}^{\mathbb{P}}(\epsilon_k^2)$ as;

$$\begin{aligned} \mathbb{E}^{\mathbb{P}}(\epsilon_k^2) &= \frac{1}{2}\Big[(1)^2\Big((1+\frac{(\mu-r)-\frac{1}{2}\sigma^2}{\sigma}\sqrt{\Delta t}\Big)+(-1)^2\Big(1-\frac{(\mu-r)-\frac{1}{2}\sigma^2}{\sigma}\sqrt{\Delta t}\Big)\Big] \\ &= 1 \end{aligned}$$

Gathering the assumptions made above, we now investigate the MGF of $X^{(N)}$ defined as;

$$\begin{aligned} M_{X^{(N)}}(\lambda) &= \mathbb{E}^{\mathbb{P}}\Big[e^{\lambda X^{(N)}}\Big] \\ &= \mathbb{E}^{\mathbb{P}}\Big[e^{\lambda\left(rN\Delta t+\sigma\sqrt{\Delta t}\sum_{k=1}^{N}\epsilon_k\right)}\Big] \\ &= \mathbb{E}^{\mathbb{P}}\Big[e^{\lambda\left(rT+\sigma\sqrt{\Delta t}\sum_{k=1}^{N}\epsilon_k\right)}\Big] \qquad \text{since} \quad \Delta t = \frac{T}{N} \\ &= e^{\lambda rT}\mathbb{E}^{\mathbb{P}}\Big[e^{\lambda\sigma\sqrt{\Delta t}\sum_{k=1}^{N}\epsilon_k}\Big] \\ &= e^{\lambda rT}\mathbb{E}^{\mathbb{P}}\Big[\prod_{k=1}^{k}e^{\lambda\sigma\sqrt{\Delta t}\epsilon_k}\Big] \\ &= e^{\lambda rT}\left(\mathbb{E}^{\mathbb{P}}\Big[e^{\lambda\sigma\sqrt{\Delta t}\epsilon_k}\Big]\right)^N \qquad \text{since} \quad \epsilon_k \quad \text{are iid} \end{aligned}$$

By second-order Taylor expansion, we expand the exponential terms as follows;

$$\begin{aligned} \mathbb{E}^{\mathbb{P}}\Big[e^{\lambda\sigma\sqrt{\Delta t}\epsilon_k}\Big] &= \mathbb{E}^{\mathbb{P}}\Big[1+\lambda\sigma\sqrt{\Delta t}\epsilon_k+\frac{1}{2}\lambda^2\sigma^2\Delta t\epsilon_k^2+o(\Delta t)\Big] \\ &\approx 1+\lambda\sigma\sqrt{\Delta t}\mathbb{E}^{\mathbb{P}}(\epsilon_k)+\frac{1}{2}\lambda^2\sigma^2\Delta t\mathbb{E}^{\mathbb{P}}(\epsilon_k^2)+o(\Delta t) \\ &= 1+\lambda\Delta t\big((\mu-r)-\frac{1}{2}\sigma^2\big)+\frac{1}{2}\lambda^2\sigma^2\Delta t+o(\Delta t) \quad \text{Based on} \quad \mathbb{E}(\epsilon_k) \quad \text{and} \quad \mathbb{E}(\epsilon_k^2) \end{aligned}$$

Now, as $N \to \infty$, we have,

$$\begin{aligned}
M_{X^{(N)}}(\lambda) &= \lim_{N\to\infty} \mathbb{E}^{\mathbb{P}}\Big[e^{\lambda X^{(N)}}\Big] \\
&= \lim_{N\to\infty} e^{\lambda r T}\left(\mathbb{E}^{\mathbb{P}}\Big[e^{\lambda\sigma\sqrt{\Delta t}\epsilon_k}\Big]\right)^N \\
&= e^{\lambda r T}\lim_{N\to\infty}\left(\mathbb{E}^{\mathbb{P}}\Big[e^{\lambda\sigma\sqrt{\Delta t}\epsilon_k}\Big]\right)^N \\
&= e^{\lambda r T}\lim_{N\to\infty}\Big[1+\lambda\Delta t\big((\mu-r)-\frac{1}{2}\sigma^2\big)+\frac{1}{2}\lambda^2\sigma^2\Delta t + o(\Delta t)\Big]^N \\
&= e^{\lambda r T}\lim_{N\to\infty}\Big[1+\lambda\frac{T}{N}\big((\mu-r)-\frac{1}{2}\sigma^2\big)+\frac{1}{2}\lambda^2\sigma^2\frac{T}{N} + o(\Delta t)\Big]^N
\end{aligned}$$

NOTE: By definition, $\lim_{n\to\infty}(1+\frac{x}{n})^n = e^x$. Using this relation, we can simplify the equation above as below,

$$\begin{aligned}
M_{X^{(N)}}(\lambda) &= e^{\lambda r T}\lim_{N\to\infty}\Big[1+\lambda\frac{T}{N}\big((\mu-r)-\frac{1}{2}\sigma^2\big)+\frac{1}{2}\lambda^2\sigma^2\frac{T}{N} + o(\Delta t)\Big]^N \\
&= e^{\lambda r T}\lim_{N\to\infty}\Big[1+\frac{\mu T\big((\mu-r)-\frac{1}{2}\sigma^2\big)+\frac{1}{2}\lambda^2\sigma^2 T}{N} + o(\Delta t)\Big]^N \\
&= e^{\lambda r T} e^{\left(\lambda T\left((\mu-r)-\frac{1}{2}\sigma^2\right)+\frac{1}{2}\lambda^2\sigma^2 T\right)} \\
&= e^{\left(\lambda T\left(\mu-\frac{1}{2}\sigma^2\right)+\frac{1}{2}\lambda^2\sigma^2 T\right)}.
\end{aligned}$$

Thus the MGF becomes $M_{X^{(N)}}(\lambda) = e^{\left(\lambda\left(\mu-\frac{1}{2}\sigma^2\right)T+\frac{1}{2}\lambda^2\sigma^2 T\right)}$, which is the Moment generating function of a normal distribution $N\big((\mu-\frac{1}{2}\sigma^2)T, \sigma^2 T\big)$, then we can conclude that,$X^{(N)}$ converges to a normal distribution as $N \to \infty$.

Hence we complete the proof that:

$$X^{(N)} \xrightarrow[N\to\infty]{d} (\mu-\frac{1}{2}\sigma^2)T + \sigma\sqrt{T}Z, \qquad \text{where} \quad Z \overset{\mathbb{P}}{\sim} \mathcal{N}(0,1)$$

□

2.2 Distribution of S_T under probabilities $\mathbb{Q}$ and $\mathbb{Q}^s$

Let $\mathbb{Q}$ refers to the martingale measure induced by using the bank account **B** as a numeraire, and $\mathbb{Q}^s$ refers to the martingale measure induced by the asset **S** as a numeraire. Based on this we shown the derivation of probabilities $\mathbb{Q}(\epsilon_k = \pm 1)$ and $\mathbb{Q}^s(\epsilon_k = \pm 1)$, as well as the $\mathbb{Q}$ and $\mathbb{Q}^s$ distribution of S_T as the limit $N \to \infty$.

Proof. Consider a risk -neutral probability with asset **B** as a numeraire, it follows from fundamental theorem of asset pricing, we require the propbability $\mathbb{Q}$ to satistfy;

$$\mathbb{E}^{\mathbb{Q}}\Big[\frac{S_t}{B_t}|\mathcal{F}_0\Big] = \frac{S_0}{B_0} \tag{1}$$

Using the theorem, we need to find the risk-neutral probabilities using the bank account **B** as the numeraire satisfies that:

$$\begin{aligned} S &= e^{-r\Delta t}\mathbb{E}^{\mathbb{Q}}(S_{\Delta t}) \\ &= e^{-r\Delta t}\Big[\mathbb{Q}(\epsilon_k = +1)Se^{r\Delta t+\sigma\sqrt{\Delta t}} + \mathbb{Q}(\epsilon_k = -1)Se^{r\Delta t-\sigma\sqrt{\Delta t}}\Big] \end{aligned}$$

Solving the equation above, we get the expressions of the PMF for ϵ_k:

$$\mathbb{Q}(\epsilon_k = +1) = \frac{1 - e^{-\sigma\sqrt{\Delta t}}}{e^{\sigma\sqrt{\Delta t}} - e^{-\sigma\sqrt{\Delta t}}}$$

and

$$\mathbb{Q}(\epsilon_k = -1) = 1 - \mathbb{Q}(\epsilon_k = +1) = \frac{e^{-\sigma\sqrt{\Delta t}} - 1}{e^{\sigma\sqrt{\Delta t}} - e^{-\sigma\sqrt{\Delta t}}}$$

Then consider switching the numeraire to asset **S**. Based on the Fundamental theorem of asset pricing,

$$\mathbb{E}^{\mathbb{Q}}\Big[\frac{B_t}{S_t}|\mathcal{F}_0\Big] = \frac{B_0}{S_0} \tag{2}$$

the risk-neutral probability satisfies that;

$$\frac{1}{S} = \frac{e^{r\Delta t}}{Se^{r\Delta t+\sigma\sqrt{\Delta t}}}\mathbb{Q}^S(\epsilon_k = +1) + \frac{e^{r\Delta t}}{Se^{r\Delta t-\sigma\sqrt{\Delta t}}}\mathbb{Q}^S(\epsilon_k = -1)$$

Thus;

$$\begin{aligned} \mathbb{Q}^S(\epsilon_k = +1) &= \frac{1 - e^{\sigma\sqrt{\Delta t}}}{e^{-\sigma\sqrt{\Delta t}} - e^{\sigma\sqrt{\Delta t}}} \\ \mathbb{Q}^S(\epsilon_k = -1) &= 1 - \mathbb{Q}^S(\epsilon_k = +1) \end{aligned}$$

Now, we can look into the limiting distribution under $\mathbb{Q}$. Since

$$Q\left(\epsilon_k = +1\right) = \frac{1 - e^{-\sigma\sqrt{\Delta t}}}{e^{\sigma\sqrt{\Delta t}} - e^{-\sigma\sqrt{\Delta t}}}$$

Applying the first-order Taylor expansion to it we have

$$\begin{aligned} Q\left(\epsilon_k = +1\right) &= \frac{1 - \left(1 - \sigma\sqrt{\Delta t} + \frac{1}{2}\sigma^2\Delta t + o\left(\Delta t\right)\right)}{\left(1 + \sigma\sqrt{\Delta t} + \frac{1}{2}\sigma^2\Delta t + o\left(\Delta t\right) - \left(1 - \sigma\sqrt{\Delta t} + \frac{1}{2}\sigma^2\Delta t + o\left(\Delta t\right)\right)\right.} \\ &= \frac{\sigma\sqrt{\Delta t} - \frac{1}{2}\sigma^2\Delta t + o\left(\Delta t\right)}{2\sigma\sqrt{\Delta t} + o\left(\Delta t\right)} \\ &= \frac{1}{2}\left(1 - \frac{\sigma\sqrt{\Delta t}}{2}\right) + o(\Delta t) \end{aligned}$$

and by generality, $Q\left(\epsilon_k=-1\right)=\frac{1}{2}\left(1+\frac{\sigma\sqrt{\Delta t}}{2}\right)+o(\Delta t)$. We noticed that the probability expression are very similar to the $\mathbb{P}$(Physical probabilities) given in part one, except that μ or the drift term is replaced by the risk-free rate r. That is $Q\left(\epsilon_k=-1\right)$ takes the form,

$$\mathbb{Q}(\epsilon_t=\pm 1)=\frac{1}{2}\big(1\pm\frac{(r-r)-\frac{1}{2}\sigma^2}{\sigma}\sqrt{\Delta t}\big),$$

Hence, we can define the MGF of $\log\left(\frac{ST}{S_0}\right)$, as:

$$\mathbb{E}^{\mathbb{Q}}\left[e^{\mu\log\left(\frac{ST}{S_0}\right)}\right]=E^{\mathbb{Q}}\left[e^{\mu X(N)}\right]=e^{urT}\left(\mathbb{E}^{\mathbb{Q}}\left(e^{\mu\sigma\sqrt{\Delta t}\epsilon_k}\right)\right)^N$$

where $E^{\mathbb{Q}}\left(e^{\mu\sigma\sqrt{\Delta t}\epsilon_k}\right)\approx 1+\mu\sigma\sqrt{\Delta t}\mathbb{E}^{\mathbb{Q}}\left(\epsilon_k\right)+\frac{1}{2}\mu^2\sigma^2\Delta t\mathbb{E}^{\mathbb{Q}}\left[\epsilon_k^2\right]=1+\mu\Delta t\left(-\frac{\sigma^2}{2}\right)+\frac{1}{2}\mu^2\sigma^2\Delta t$

As $N\to\infty$,

$$\begin{aligned}&\lim_{N\to\infty}\left[\mathbb{E}^{\mathbb{Q}}\left(e^{\mu\sigma\sqrt{\Delta t}\epsilon_k}\right)\right]^N\\&=\exp\left(\mu T\left(-\frac{1}{2}\sigma^2\right)+\frac{1}{2}\mu^2\sigma^2T\right)\end{aligned}$$

So the MGF of $X^{(N)}$ is

$$\begin{aligned}\mathbb{E}^{\mathbb{Q}}\left[e^{\mu X(N)}\right]&=e^{\mu rT}\exp\left(\mu T\left(-\frac{1}{2}\sigma^2\right)+\frac{1}{2}\mu^2\sigma^2T\right)\\&=\exp\left(\mu T\left(r-\frac{1}{2}\sigma^2\right)+\frac{1}{2}\mu^2\sigma^2T\right)\end{aligned}$$

Which is the MGF of Normal distribution with mean $\left(r-\frac{1}{2}\sigma^2\right)T$ and variance σ^2T. Since the function is continuous, we can conclude from Levy's continuity theorem that $\log\left(\frac{S_T}{s_0}\right)\underset{N\to\infty}{d}N\left(\left(r-\frac{1}{2}\sigma^2\right)T,\sigma^2T\right)$ as the number of subperiods tends toward infinity. The limiting distribution of S_T is lognormal: $S_T\xrightarrow{d}S_0\exp\left[\left(r-\frac{1}{2}\sigma^2\right)T+\sigma\sqrt{T}Z\right]$, where $Z\overset{\mathbb{Q}}{\sim}(0,1)$

Let's look at the limiting distribution under $\mathbb{Q}^S$. We know,

$$\mathbb{Q}^S\left(\epsilon_k=+1\right)=\frac{1-e^{\sigma\sqrt{\Delta t}}}{e^{-\sigma\sqrt{\Delta t}}-e^{\sigma\sqrt{\Delta t}}}.$$

Applying first-order Taylor expansion

$$\begin{aligned}&=\frac{1-\left(1+\sigma\sqrt{\Delta t}+\frac{1}{2}\sigma^2\Delta t+o\left(\Delta t^{3/2}\right)\right.}{\left(1-\sigma\sqrt{\Delta t}+\sigma^2\Delta t+o\left(\Delta t^{3/2}\right)\right)-\left(1+\sigma\sqrt{\Delta t}+\sigma^2\Delta t+o\left(\Delta t^{3/2}\right)\right)}\\&=\frac{-\sigma\sqrt{\Delta t}-\frac{1}{2}\sigma^2\Delta t+o\left(\Delta t^{3/2}\right)}{-2\sigma\sqrt{\Delta t}+o\left(\Delta t^{3/2}\right)}\\&=\frac{1}{2}\left(1+\frac{\sigma\sqrt{\Delta t}}{2}\right)+o(\Delta t)\end{aligned}$$

and $\mathbb{Q}^S(\epsilon_k = -1) = \frac{1}{2}\left(1 - \frac{\sigma\sqrt{\Delta t}}{2}\right) + o(\Delta t)$. Comparing $\mathbb{Q}^S$ to $\mathbb{Q}$ before, we can use the same process to get the MGF of $X^{(N)}$ under $\mathbb{Q}^S$ measure is:

$$E^{Q^s}\left[e^{\mu X(N)}\right] = \exp\left[\mu T\left(r + \frac{1}{2}\sigma^2\right) + \frac{1}{2}\mu^2\sigma^2 T\right]$$

Which is the MGF of Normal distribution with mean $\left(r + \frac{1}{2}\sigma^2\right)T$ and variance $\sigma^2 T$. Since the function is continuous, we can conclude from Levy's continuity theorem that: $\log\left(\frac{S_T}{S_0}\right) \xrightarrow[N\to\infty]{d} N\left(\left(r + \frac{1}{2}\sigma^2\right)T, \sigma^2 T\right)$ under the probability $\mathbb{Q}^s$ and $S_T \xrightarrow{d} S_0 \exp\left[\left(r + \frac{1}{2}\sigma^2\right)T + \sigma\sqrt{T}Z\right]$, where $Z \overset{\mathbb{Q}^s}{\sim} N(0,1)$. Hence the proof of the two cases is completed. □

3 Results

3.1 Implementation of the American Put option

In this part, we implemented a 5000 steps American put option using binomial tree model and considering the parameters $T = 1, S_0 = 10, \mu = 5\%, \sigma = 20\%$ and $r = 2\%$. The up and down movement of the prices using the binomial tree method applies the Bernoulli probabilities defines as,

$$p = \frac{e^{r\Delta t} - e^{-\sigma\sqrt{\Delta t}}}{e^{\sigma\sqrt{\Delta t}} - e^{-\sigma\sqrt{\Delta t}}}$$

where $\triangle t = T/N$ is the length for each time step. We caculate the prices in each binomial trade where each node represents time period and price of the asset at that time. Let i denote the time period t and j represent the the j^{th} possible prices where $i \in [0, 5000], j\epsilon[0, 5000]$ where in this case 5000 is the number of simulations. Let node $[i, j]$ be $S_{i,j}$, then the price in the next period is given as,

$$S_{i+1,j} = S_{i,j} * e^{\sigma\sqrt{\Delta t}} \quad , \qquad S_{i+1,j+1} = S_{i,j} * e^{-\sigma\sqrt{\Delta t}}$$

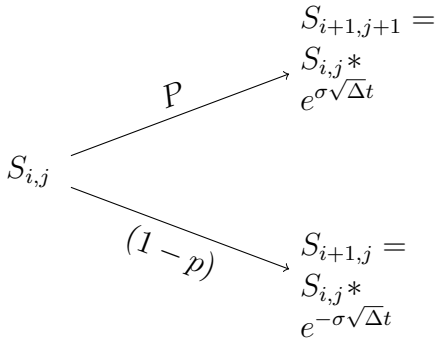

To determine the exercise boundary, we first calculated the option's value at each node. Normally, the option value $V_{i,j}$ for American put option at each node is calculated as,

$$V_{i,j} = \max\left(K - S_{i,j}, 0\right)$$

To decide the early exercise boundary, the fairly option value $V^*_{i,j}$ on each node was calculated as the discounted value of the two option values in the preceding period. That is,

$$V^*_{N,j} = V_{N,j}$$

$$V^*_{i,j} = e^{-r\Delta t} * \left[q * V^*_{i+1,j} + (1-q) * V^*_{i+1,j+1}\right]$$

If the option value $V_{i,j}$ was higher than the calculated fairly option value, then the American put option was early exercised otherwise it was held.

$$V_{i,j} = \max\left(V_{i,j}, V^*_{N,j}\right)$$

By definition, an exercise boundary is a boundary between early-exercise area and non-early-exercise area [1]. Therefore, the boundary is formed by points with highest stock price at different same time steps which can be early-exercised. In the figure below, we demonstrate the plot of the exercise boundary as function of time t;

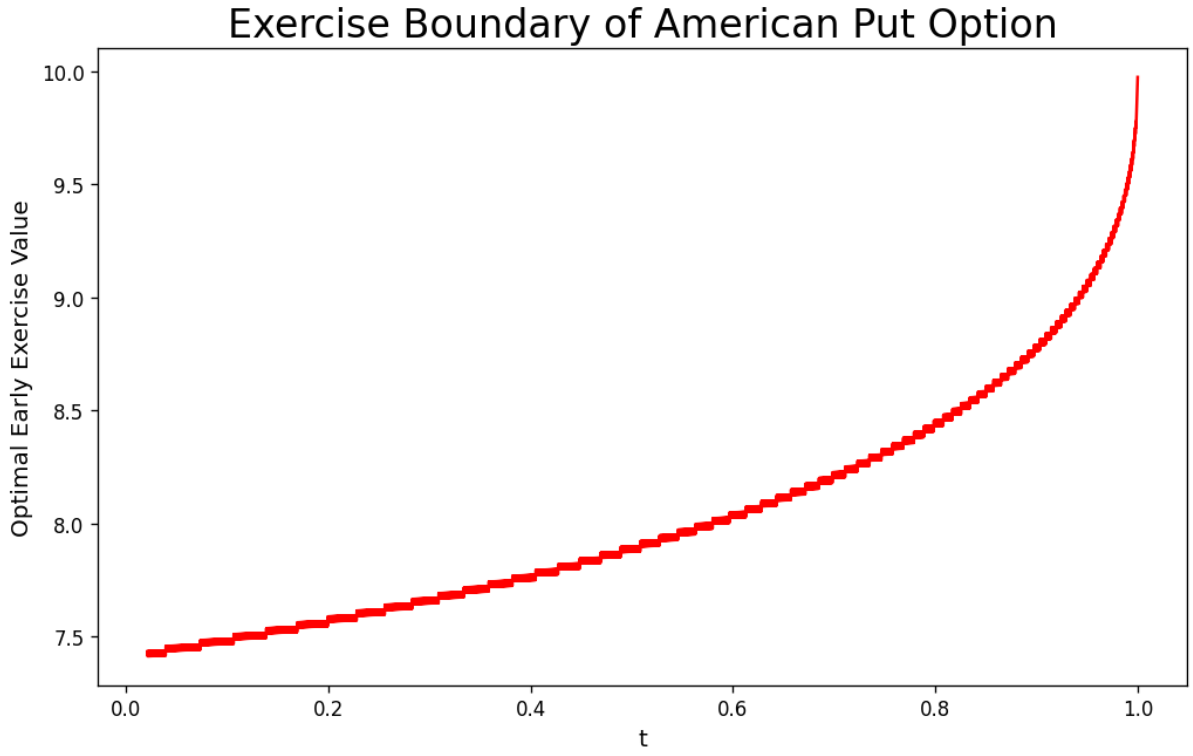

Figure 1: Exercise Boundary of American Put Option

We can see from the figure above that the exercise boundary exhibits the distinctive curve for the American options with the exercise values being low during earlier times and higher at times nearing maturity. The region that is below the boundary is the exercise region and the region above the boundary is the "hold" region where one does not call for

an early exercise. The plot suggests that for times at the start of the contract, it would be hard for the asset to start at price 10 then to immediately dip down to the exercise boundary.

After that we implemented different hedging strategy with respect to the spot price of the underlying asset at several time points. This is further illustrated in the figure below.

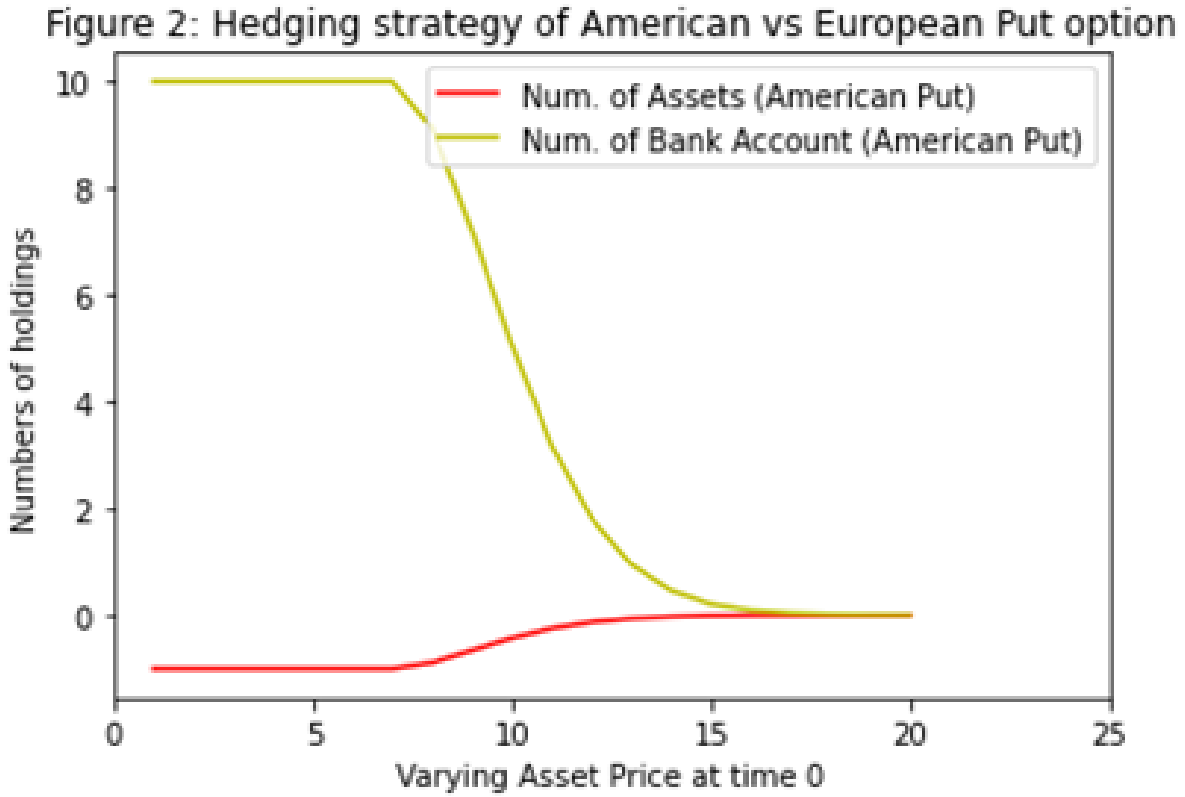

Figure 2: Hedging strategy of American vs European put option

As the Figure(2) shows the hedging position for American and European option at time $t = 0$ if the initial asset price varying between 1 and 25, given other parameters are the same. It is clearly shown that the two lines, representing the numbers of risky asset and risk-free asset to be hold at time $t = 0$ respectively converge to zero when the underlying stock price reaches 18 from different directions and stay level afterwards. This indicates that investors should short one risky asset and long 10 units of risk-free asset when the initial stock price is lower than 8 to construct a hedging portfolio. They shall reduce their holdings of both asset when the initial stock price is higher than 8.

One thing to note is that if we do not consider the initial underlying asset price would change, the hedging position at time $t = 0$ given initial asset price equals to 10 should be -0.436 units of risky asset and 5.068 units of risk-free asset. This will be shown as a point in the graph below;

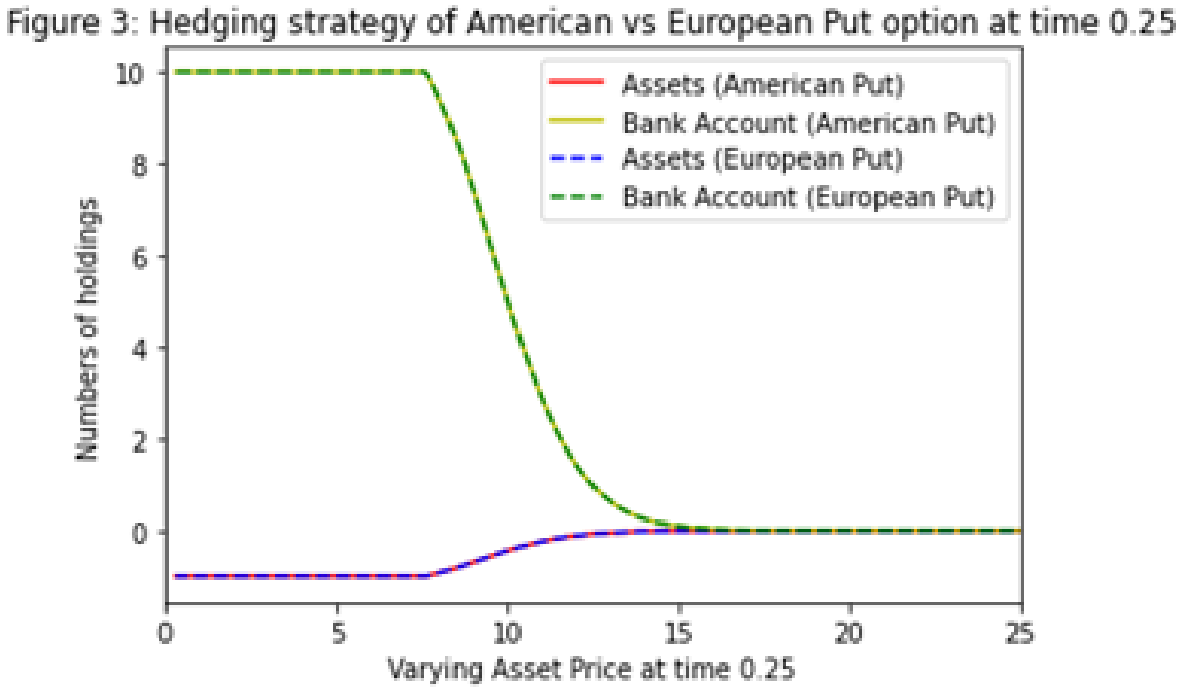

Figure 3: Hedging strategy of American vs European put option at time 0.25

To visualize the hedging strategy for at different time points, we generated the units of each asset to be hold at time = 0.25, 0.5, 0.75 and 1 with respect to the price of the underlying asset at each time. The Figure (3) above displays the change of the hedging portfolio at time = 0.25 as the underlying asset price vary from 0 to 25. It is obvious that the hedging curves are very similar to the ones at time = 0. The lines represent the hedging strategy of a European Put with same risk parameters is also plotted. Since the chance to exercise the American option is low at this timepoint, the hedging position of American and European options are close, and the difference is unobvious to observe from the graph. As the asset price increases up to 8 at time = 0.25, the units of risky assets and risk-free asset remain level at -1 and 10 respectively, indicating that the investors shall short 1 risky asset and long 10 risk-free assets to hedge the put option. When asset price increases to 15, the unit of risky asset smoothly increases while the unit of risk-free asset quickly drops. They converge at 0 and remained constant as the asset price increases furthermore.

The hedging curve at time = 0.5, 0.75 and 1 were also computed and visualized. Since they have similar shapes and trends, we plot them in the same plot for clear comparison.

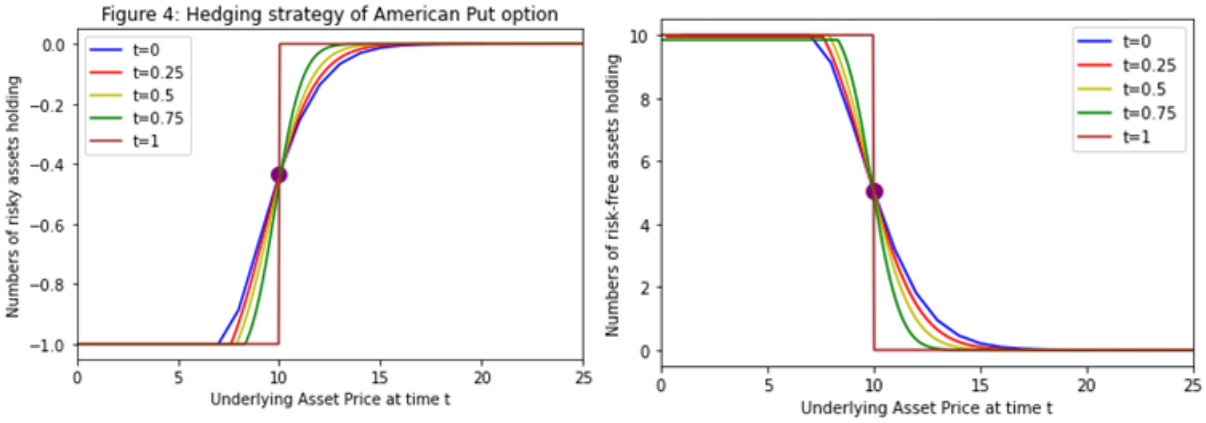

Figure 4: Hedging strategy of American Put Option

The Figure(4) above show the holdings patterns of risky and risk-free assets respectively in the hedging portfolio. The solid round point with the coordinates (10, -4.36) and coordinates (10, 5.068) in Figure(4) represents the hedging position when the initial underlying stock price is set to fixed at 10, investors should short 4.36 units of the risky asset and long 5.068 units of the bank account asset to replicate the payoff of this American Put option in the future state.

The curve in the graph has homogeneous pattern across the different time points at 0, 0.25, 0.5 and 0.75. Hence, the hedging strategy at each of these four time point will be alike to the ones at time = 0 and time = 1 that we have suggested in the previous discussion. The replicating portfolio at time t = 1 is different from the time points prior to it since it is evaluated at the maturity date that future payoff does no longer exist. At time = 1, investor will exercise the put option by selling a stock if the stock price is lower than the strike price 10. The hedging strategy under this circumstance is to long 10 units of the Bank Account asset so that the total cashflow at time = 1 equals to 0. Otherwise, if the stock price is higher than the strike price at time = 1, the investors choose not to exercise the option and consequently no hedging strategy will be performed.

We further explored the characteristics of the decision boundary as market conditions changed. First, we investigated the behaviour of the decision boundary with the variation of the σ. The output of the exploration is illustrated in the figure below;

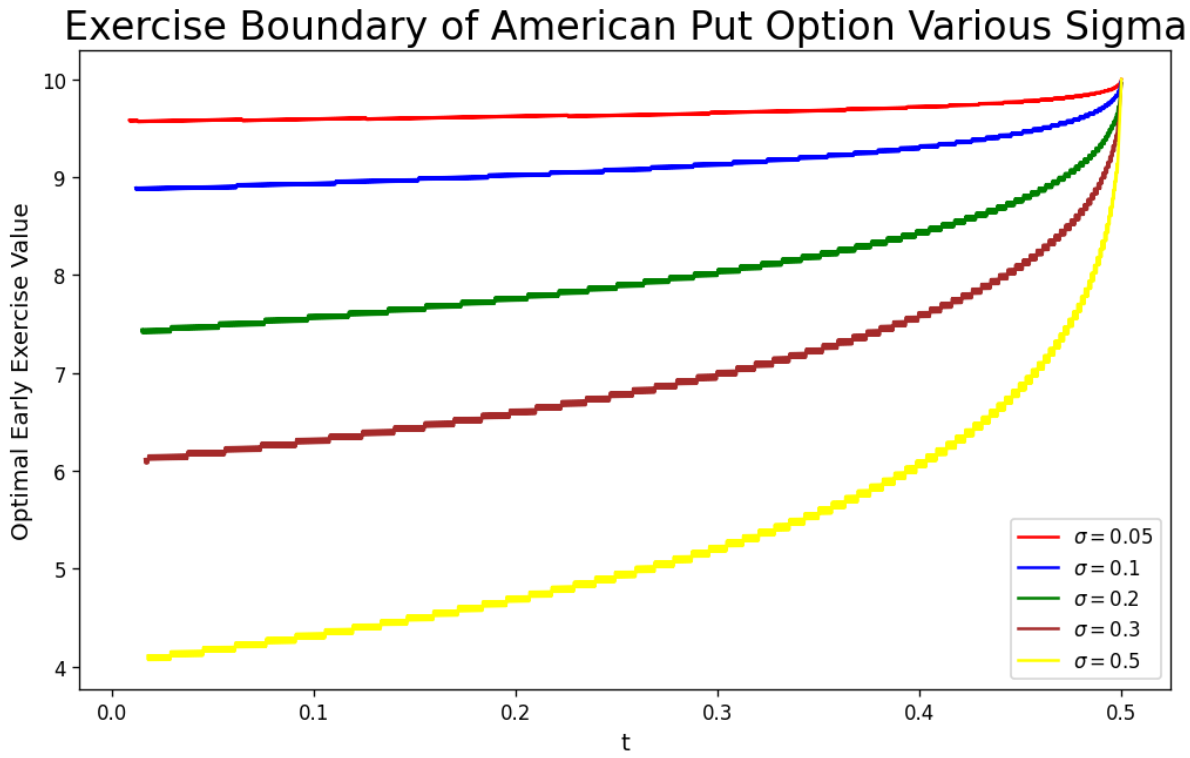

Figure 5: Decision boundaries with varying Volatility(σ).

From the above figure, we can see that, as the σ value varies, the shape of the decision boundary also varies. These variations are correlated directly with the level of volatility. This is due to the volatility being used for the calculation of the risk-neutral probability which we had discussed earlier and directly affects the direction of the risk-neutral. The results of the decision boundaries coincide with the notion of volatility. We can see that as σ is higher, we can see that the decision to exercise is relatively lower during the early time compared to when σ is higher. We can also see that as time goes on, the probability to exercise all rise and converges as time approaches maturity. Note that with extremely low market volatility, the exponential curve of the decision boundary becomes less noticeable.

We now explore some other variables to see their effects on the decision boundary.

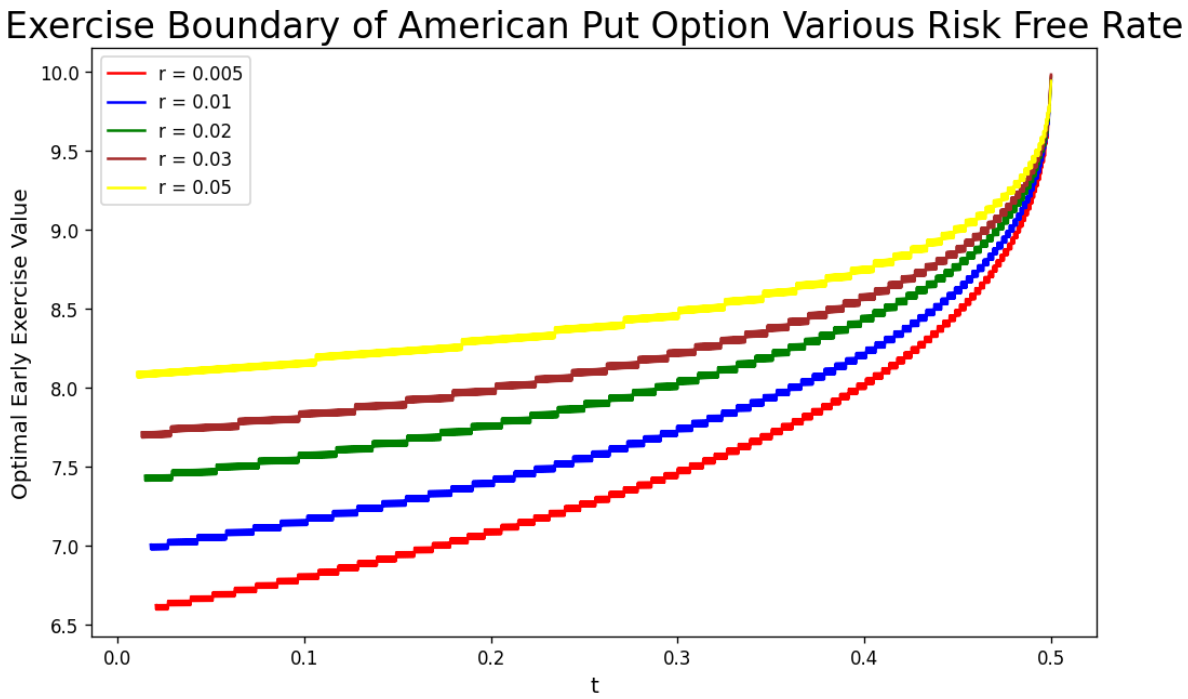

Figure 6: The American option exercised at various Risk-free rates

Above, we can see the shape of the decision boundaries are also influenced by different risk-free rates since the risk-free rate is also used for calculating the the risk-neutral probabilities. We see that with higher risk-free rates, the market has higher early exercise values than that of the lower risk free rates while the inverse can be said for lower risk-free rates leading to lower early exercise values. This implies that having a lower risk-free rate would lead to lower probabilities that an early exercise value close to $t = 0$.

The next step analyzes the change exercise boundary and hedging strategy of the American Put option when giving different volatility and risk-free rates.

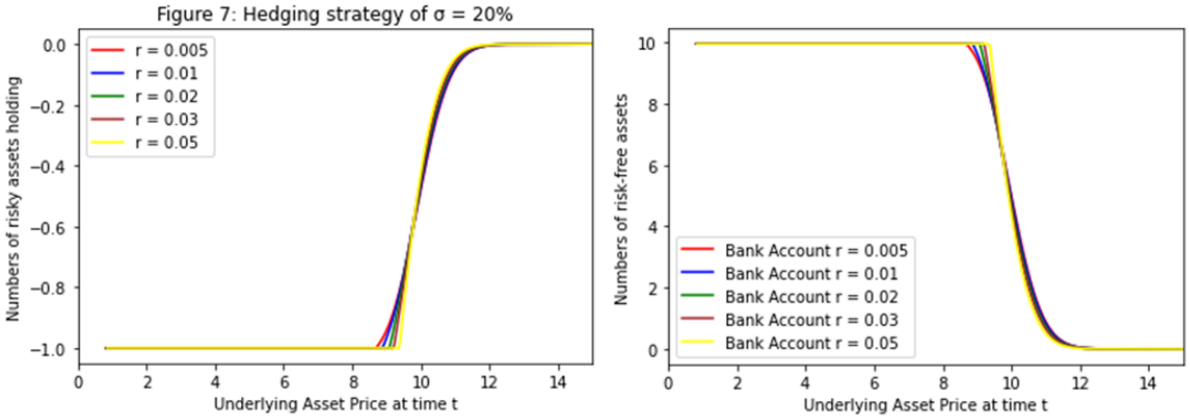

Figure 7: Hedging strategy under $\sigma = 20\%$.

To analyse the influence of risk-free rate, we set $r = 0.5\%, 1\%, 2\%, 3\%, 5\%$ and keep the other parameters unchanged. Figure 7 shows the comparison of hedging position

generated at time point 0.25 when risk-free rate varies from 0.5% to 5%. The curve of risky and risk-free asset with respect to the underlying stock price at time = 0.25 do not display a significant variation. Since risk-free interest rate affect the of risk-neutral probability and discounting factor of option value at each node, it does not affect the movement factor of stock price and hence does not have a substantial impact of the underlying asset price at future time points. According to the equation used to solve for the number of holdings to each asset, the hedging position is more dependent on the movement of the stock price. Therefore, the hedging strategy of an American put option as a function of the spot price S is not strongly affected by variation of the risk-free rate.

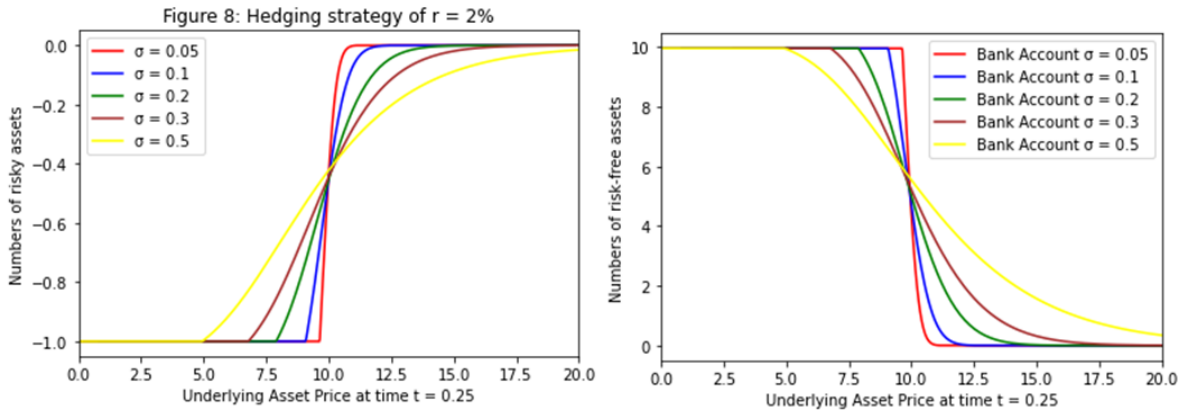

Figure 8: Hedging strategy of $r = 2\%$.

To analyse the influence of risk-free rate, we let $\sigma = 5\%$, 10%, 20%, 30%, 50% and keep risk-free rate remains to be 2%. Figure 8 shows the comparison of hedging position generated at time point 0.25 when volatility varies from 5% to 50%. For high volatility the units of risky assets to short and bank account assets to long starts to decrease when the underlying stock price rises above 5, which is the lowest compared to the low volatility scenarios. Since Volatility determines the risk-neutral probability as well as the magnitude that underlying stock price moving up or down. High volatility leads to the greater variation in the future stock price, meaning that the option has a higher risk compared to the others with low volatility. Therefore, investors tend to adopt a hedging strategy with less risky asset to short as well as less risk-free asset to long.

Now that we have the exercise boundaries and hedging strategies at various times, let us observe some simulations of price paths. We choose ten-thousand sample paths to simulate all with five thousand time steps to get a more complete view of the implications of the profits and loss at the boundary condition.

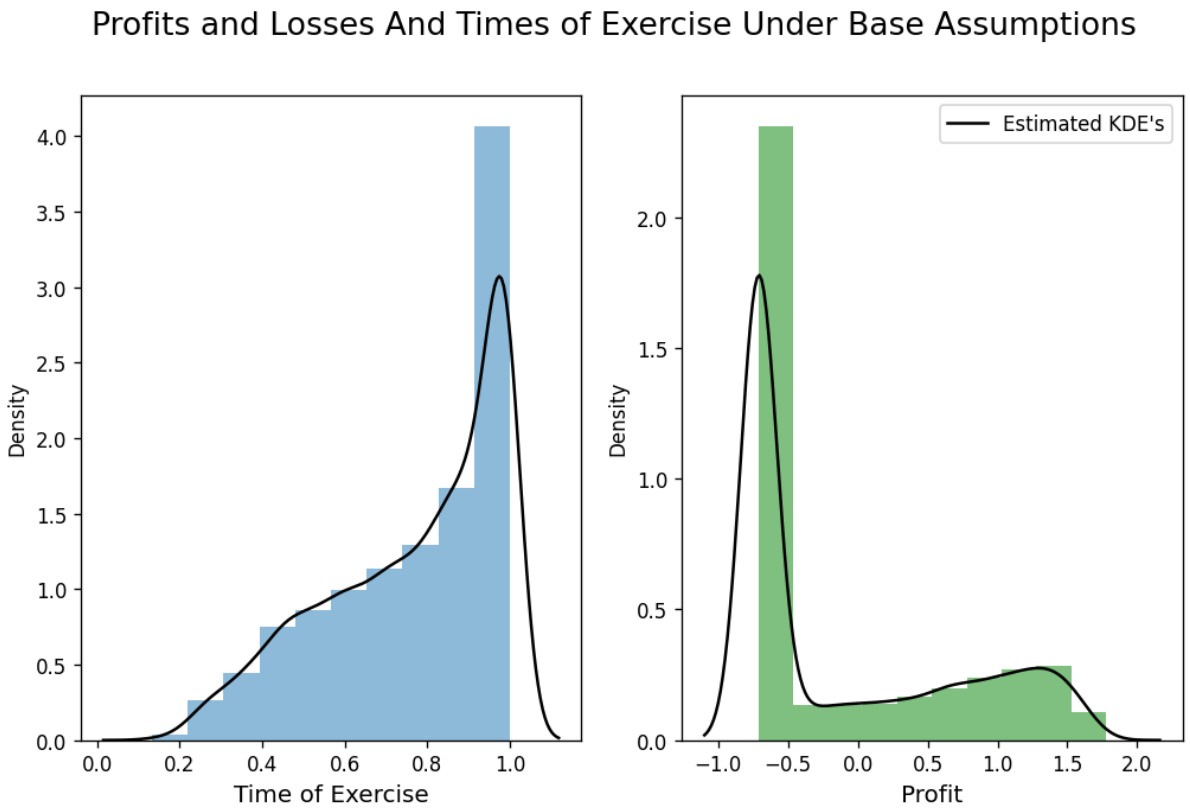

Figure 9: Kernel Density estimates of time of exercise and profit

Above, we see the histograms and their estimated kernel density of the profits/loss that incurred at exercising at the decision boundary. The plot on the left is the distribution of the times that the option was exercised. We can see that like the shape of the decision boundary, the decision to exercise early is low at earlier times and the number of options exercised later on nearing maturity.

On the right, we see the profits of all the options that were exercised early or not at all. This is why we see large counts of profits around -0.7 which is the valuation of the contract given that the option was not exercised at all. The right plot also suggests that when a option is exercised early, more times than not there was profit to be made. However, this is overshadowed by the overwhelming number of options that were not exercised early at all which leads to the guaranteed loss.

Let us now observe how different parameters of the market affects the time of exercise and the distribution of the profits.

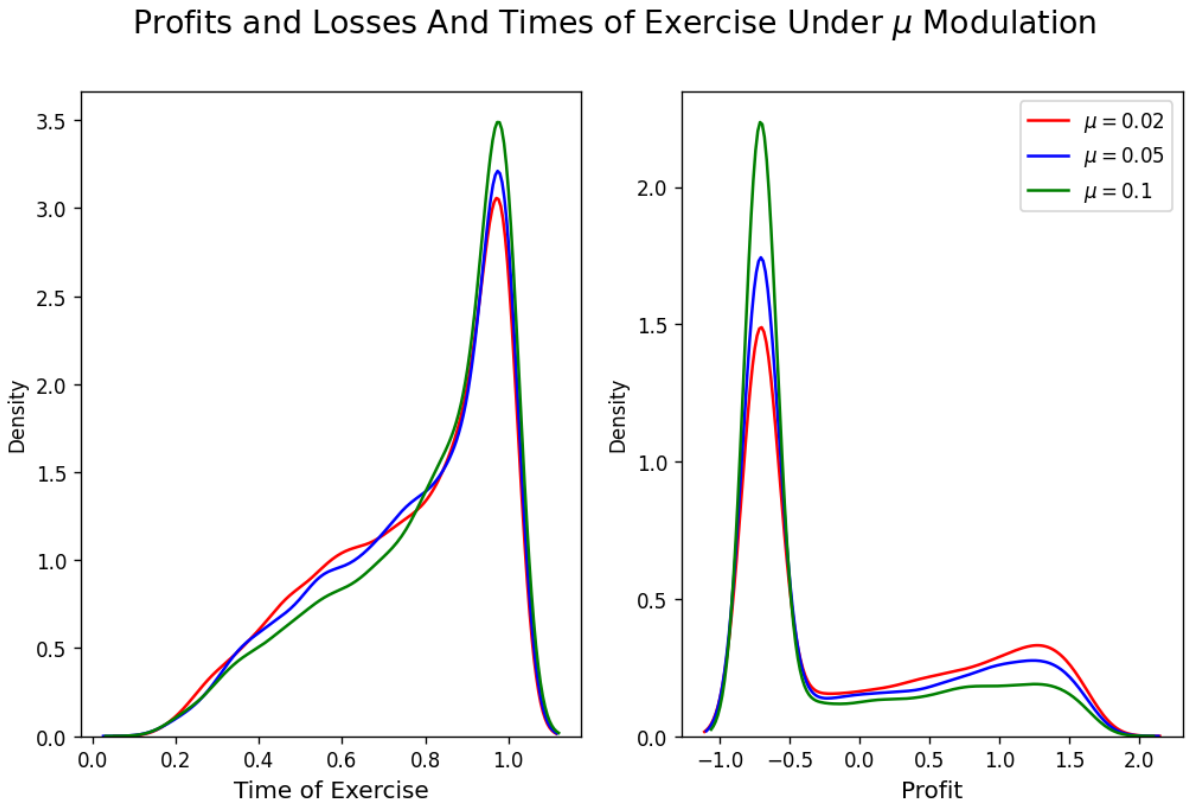

Figure 10: Profits and Losses and times of exercise under μ Modulation

Above we have the the times of exercise and the profits with each simulated path as an estimated distribution. For both plots, we have that the distribution of the original market conditions are coloured in blue.

From the time of exercise, we see that as μ decreases, the times of exercise get distributed more close to $t = 0$ which means that more options are exercised early. We can see that this notion is reflected in the profit distributions where the less the drift is, the less options are left un-exercised. The converse can be said about increased market drift (in the positives). As drift increases, more options are left un-exercised and time of exercised and more of the proportions of the profits are distributed with the non-exercising loss in contrast to the right tails that have a positive profit.

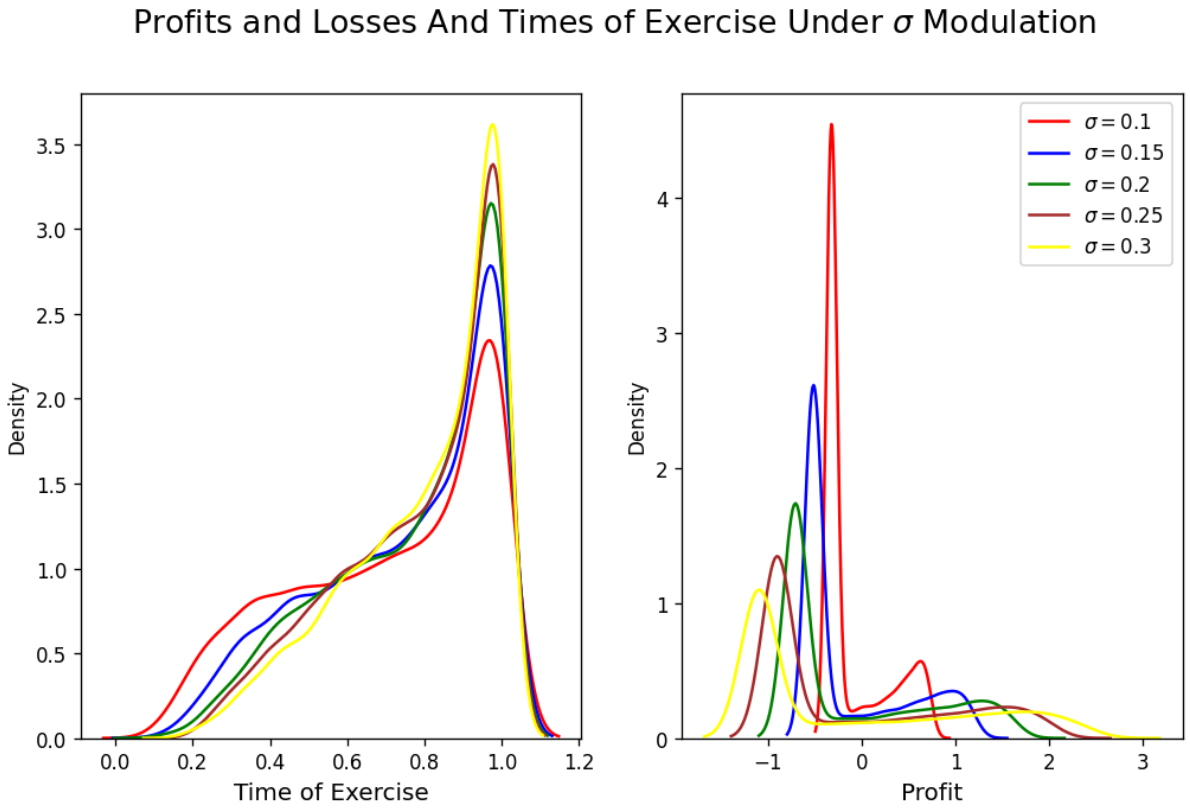

Figure 11: Profits and Losses and times of exercise estimates under various σ Modulation.

Next, we visit the interesting notion of changing market volatility. Above we have the plots of the estimated distributions of the time for exercise on the left and for profit on the left. For comparison, the results of the simulations for original market conditions are coloured in green.

The right plot suggests that higher volatility makes it easier to profit more on an option compared to lower profits as the distribution covers a larger interval on the profit axis. However, it comes at a cost where the losses can be much more severe if one were not to exercise i.e. the rate of having a more lucrative profit is also increased. The inverse can be said for a lower market volatility where despite having a lower risk of a heavy loss, the peak of the distribution suggests that the market is less likely to reach a scenario where an early exercise is optimal.

The left plot suggests that scenarios of earlier early exercise conditions are frequent with lower market volatility, however this is offset by the profits being relatively lower compared to the high volatility.

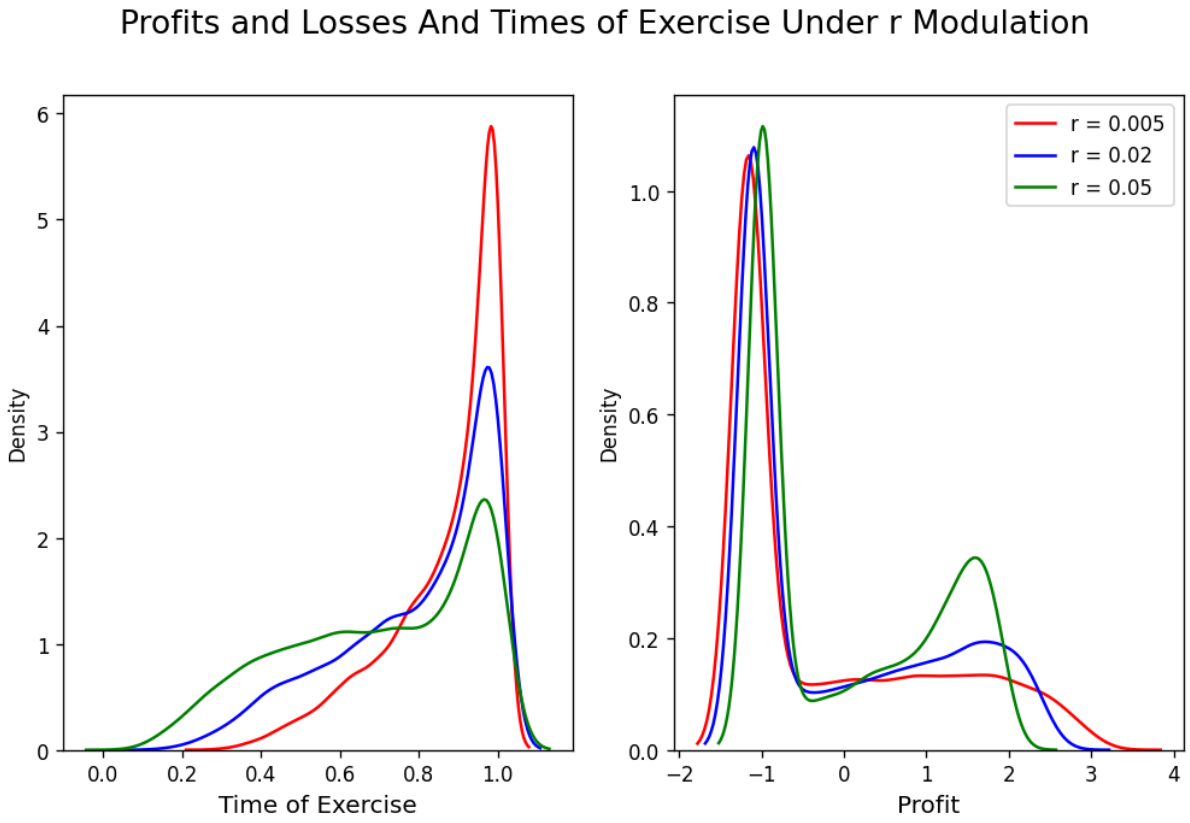

Figure 12: Profits and Losses and times of exercise estimates under r Modulation.

Finally, we observe the effects of the risk free rate on profits and loss and times of exercise.

When examining the effect of the risk-free rate on the distribution of exercise time and profits, the plot above seems to display an effect inverse of that the volatility had. Higher risk-free rates lead to a more evenly distributed exercise times away from the maturity date which is the opposite effect that a low risk-free rate has which most of its values distributed near maturity. We can see that the penalties for not exercising early at all are somewhat mitigated by having a higher risk free rate as the peaks from default losses from not exercising seem to increase slightly closer towards zero. The right plot suggests that with a lower risk-free rate, the possibility of having a higher profit is more likely than that of higher risk-free rates.

4 Conclusion

In this project we have demonstrated the limiting distribution of an asset price under both the physical probabilities($\mathbb{P}$) and risk-neutral probabilities of ($\mathbb{Q}$ and $\mathbb{Q}^s$). This gave us an hands on experience and practice of the Fundamental Theorem of Asset pricing and its assumptions made under arbitrage-free markets such as construction of martingale probabilities. We then further investigated the pricing of an American put option with an implementation Python where we used the binomial tree method to determine price the option and evaluated the option's exercise boundary as a function of time. We then varied different parameters such as the volatility(σ) and risk-free interest(r) and discussed observations on how the variations affected the option's exercise boundaries and hedging strategies for a few equally spaced time periods. We concluded the project by Simulating 10,000 sample paths of the asset and obtained kernel density estimates of the profits and losses along with the distribution of the time at which option was exercised and then Explored how the various model parameters effected these distributions.

We noted that, the American put option's exercise boundary decreased with increase in volatility(σ) and decreased with the increase in risk-free interest(r). The motivation behind this relationship can be attributed to risk-neutral being calculated with both of these values. We then saw the relationship of how hedging strategies varied with the change of market parameters at various time points before maturity. Finally, we discussed how changes in the KDE of exercise time and profit/loss at time of exercise were affected by σ, r , and μ.

References

[1] J. Sebastian and A.-A. Ali, *Pricing theory*. Unpublished-MFI, 2019.